



Role of red mud as a cementing material in concrete: a comprehensive study on durability behavior

Chava Venkatesh¹ · Ruben Nerella¹ · Madduru Sri Rama Chand²

Received: 7 July 2020 / Accepted: 12 September 2020 / Published online: 1 October 2020
© Springer Nature Switzerland AG 2020

Abstract

Red mud (RM), a semi-solid residual of the alumina refinery process, has higher alkalinity, and its disposal leads to environmental imbalance. To overcome this issue, RM is partially replaced with cement in the range of 0% to 20% at an interval of 5%. The present research work majorly focused on durability and micro-level concrete studies containing pre-calcined (600 °C in 2 h) RM. The tests on red mud concrete, viz. compressive strength, sorptivity test, open porosity test, rapid chloride penetration test, accelerated corrosion test, water absorption test, X-ray diffraction, scanning electron microscope (SEM), and energy-dispersive spectroscopy (EDS) analysis, have been conducted to investigate the comprehensive characterization of concrete with RM. From the compressive strength test results, maximum strength was observed at 10% replacement. Open porosity, chloride ions permeability, water absorption, and sorptivity values showed reduction at an increment of RM replacement level. RM concrete offered more corrosion resistance due to high alkalinity, which possessed a pH of more than 12.5. From the micro-level investigations such as SEM and EDS, higher C–S–H gel formation was observed in RM 10% replacement concrete. In the meantime, less number of pores was observed in all RM replaced concrete mixes.

Keywords Accelerated corrosion test · Durability properties · Red mud · Open porosity test · Sorptivity test · XRD

Introduction

In the alumina refinery process, raw bauxite ore is treated with concentrated NaOH solution at high pressure; thus, the semi-solid residuals are disposed off from filters, which was considered as “red mud (RM).” In the production of one ton alumina, nearly 1.5 to 2 tons of RM is disposed off, resulting in 140 million tons per annum worldwide [1]. RM, due to the presence of a higher percentage of sodium hydroxides, possesses greater alkalinity, and disposal of such material leads to rigorous ecological issues. At present, alumina industries are following the pond disposal, sea

disposal, lagooning disposal, and dry stacking methods for disposal of red mud; however, it creates some of the major environmental issues [2–5]. The solution to surmount this problem has been addressed by a few researchers who suggested utilizing the unprocessed or processed red mud as a raw material in various construction industries like brick industries and ceramic-based industries [6–9].

Very few studies were conducted on red mud as supplementary cementitious material in concrete, and the additional benefit of this industrial by-product with cement replacement was understood. There are mixed opinions on the optimum dosage of red mud in cement and its applications; Sawant et al. [10] reported that red mud could be replaced in cement up to 25%. At the same time, Metilda et al. [6] reported that red mud could be replaced up to 15%. Some other studies reported only 2% of red mud could be replaced into the cement [11]. Reason for these mixed opinions is due to the variation of chemical composition of red mud with location. Red mud, rich in alumina content, fastens the setting time of concrete and reduces compressive strength with an increased level of replacements [12]. Yang et al. [13] reported that compressive strength was increased with 6% of red mud replacement in

✉ Ruben Nerella
rubennerella2512@gmail.com

Chava Venkatesh
chvenky288@gmail.com

Madduru Sri Rama Chand
maddurusriram@gmail.com

¹ Civil Engineering, Vignan’s Foundation for Science Technology and Research, Guntur, AP, India

² Sree Chaitanya College of Engineering, Karimnagar, Telangana, India

concrete; this might be due to the densification of microstructure and which was confirmed by the reduction of calcium hydroxide content with red mud replacement.

Red mud particles have a high specific surface area (SSA), which can occupy micropores and cracks present in the concrete, thus create concrete as very dense and offer more resistance against chlorides and other gases passage into the concrete [14]. Red mud could trap the chloride ions passage and reduce its penetration into the concrete due to the red mud's higher alumina percentage [15]. Additionally, red mud in concrete improved the CSH formation, which retained carbon dioxide penetration [16]. Ribeiro et al. [17] investigated the corrosion potential of red mud-based reinforced concrete and proposed that increase in red mud content enhanced the corrosion resistance of concrete. Some of the studies identified the added advantage of red mud as a corrosion inhibitor in concrete while it reduces the Cl⁻ to OH⁻ ratio at the interface between concrete and rebar [18, 19].

As per existing literature, most of the studies used non-calcined red mud, which was only suitable for non-structural applications [20]. However, red mud's structural application was brought into the picture by the calcination method for deriving red mud's cementitious activity. When red mud particles were heated in the range of 400–900 °C, red mud particles were poorly crystallized at 600 °C and resulted in good cementitious activity [21–23]. In the present project work, red mud was heated in 600 °C temperature in various time intervals (1 h to 6 h with a constant interval of 1 h) and conducted various physical and chemical, and cementitious activity tests. Based on the investigation, 600 °C for 2 h samples showed the best performance than other samples, which was the reason for adopted 600 °C for 2 h of pre-calcined red mud used in concrete mixes.

As per available literature, there is a need to assess the red mud-based concrete's long-term behavior. The present study was performed for various mechanical, durability, and microstructural property assessment tests to fill this research gap. In the present work, red mud was pre-calcined at 600 °C for 2 h; pre-calcination converts aluminates and silicates present in red mud into alumina and reactive silica, and these formations can trigger the pozzolanic activity. Another reason is to reduce the hydroxide content, which creates hazards. Red mud was partially replaced with cement in the range of 0%, 5%, 10%, 15%, and 20% by weight of cement. X-ray diffraction (XRD) and X-ray fluorescence (X-RF) techniques were used to determine red mud's chemical properties. To understand the durability behavior of red mud concrete, the following tests were performed; sorptivity test, rapid chloride permeability test, open porosity test, and accelerated corrosion tests were conducted. Red mud concrete morphology was identified from scanning electron

microscopy (SEM) equipped with energy-dispersive spectroscopy (EDS) analysis.

Materials and methods

The present work used Type I cement conforming to ASTM C150-19 [24]. The specific surface area of cement was 330 m²/kg, evaluated by Blaine's air permeability method, and the specific gravity of cement was 3.12, evaluated according to IS 4031-1996 [25]. The crushed granite stones of 20 mm well graded were used as coarse aggregates (CA), and natural river sand was used as fine aggregates (FA) conformed to Zone-II as per IS 383:2016 [26] as shown in Table 1. Superplasticizer was used as a high water reduction agent; sulphonated naphthalene-based polymers, according to ASTM C 494:2019 [27].

Red mud

Red mud is a disposed waste from alumina refinery plants; in the present study, it was procured from the red mud disposal pond, NALCO, Damanjodi, India. At the procured stage, red mud was in the form of a semi-solid condition. The fine red mud particles were obtained by sun-drying and crushing solids particles using a ball mill. Subsequently, red mud particles were thermally treated in a muffle furnace at 600 °C for two hours. Specific gravity and specific surface area of red mud were 2.46 and 22,000 m²/kg, respectively. The chemical composition of red mud and cement is presented in Table 2, while the particle size distribution of red mud and cement particles is depicted in Fig. 1. Gibbsite, calcium carbonate, hematite, muscovite, and quartz are majorly traced mineral compositions in red mud derived from XRD analysis, as shown in Fig. 2. SEM image shown in Fig. 3 acknowledged the poorly crystallized nature of red mud particles.

Table 1 Sieve analysis of fine aggregates

IS sieve	% Of cumulative passage	
	Test results	Standard range for Zone-II
10 mm	100	100
4.75 mm	95	90–100
2.36 mm	80	75–100
1.18 mm	45	55–90
600 µm	20	35–59
300 µm	7	8–30
150 µm	0	0–10

Table 2 Chemical composition of red mud and cement evaluated by X-Ray fluorescence analysis

Material	CaO	Al ₂ O ₃	Fe ₂ O ₃	SiO ₂	Na ₂ O	MgO	K ₂ O	TiO ₂	Others
Cement	65.29	4.73	3.95	20.93	0.29	1.43	0.36	–	3.02
Red mud	9.90	21.24	22.79	23.90	5.83	0.35	2.49	5.50	8

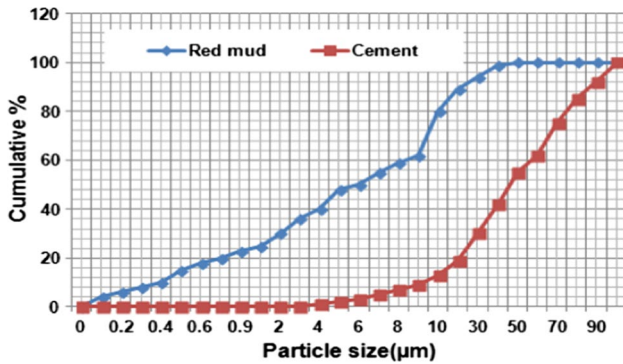


Fig. 1 Particle size distribution of red mud and cement

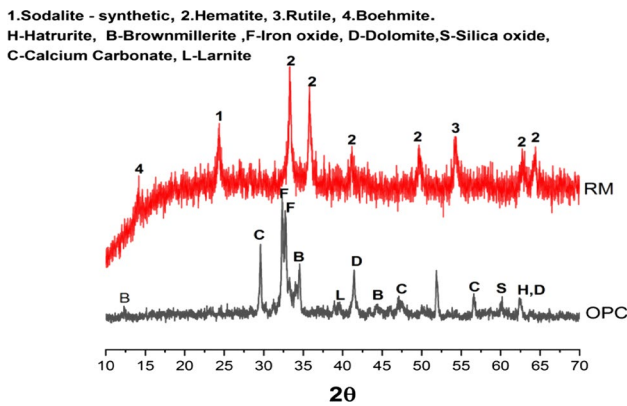


Fig. 2 X-ray diffractograms for red mud and cement

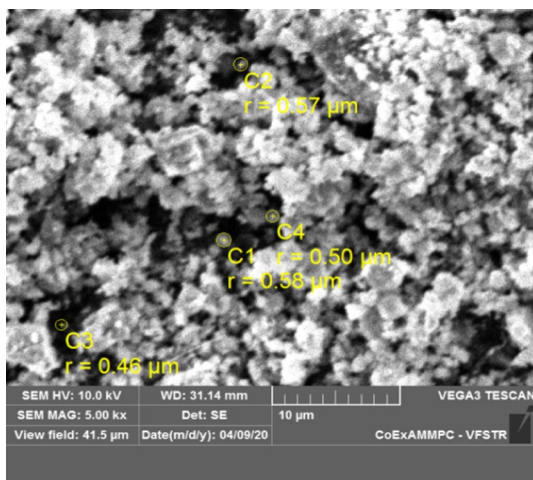


Fig. 3 SEM image of red mud

Mix proportions

Table 3 represents the mix calculations of the present study prepared as per IS 10262-2019 [28]. The study considered two mixes of standard grade (Mix A) and high strength grade (Mix B) as per IS 456-2000 [29]. The control mix was considered with 0% replacement of red mud, and further four mixes were considered with the level of replacement as 5%, 10%, 15%, and 20% by weight of cement. Mix B-based concrete was added with silica fume (SF) to achieve high-grade concrete.

Compressive strength

As per BS 12390-3: 2009 [30], red mud concrete’s compressive strength has been evaluated. The size of samples 150×150×150 mm was prepared and tested in a compressive testing machine.

Durability tests

Rapid chloride penetration test

Rapid chloride penetration test (RCPT) was conducted as per ASTM C1202-12 [31] to determine red mud concrete’s electrical conductivity. The samples’ sizes are 50 mm thickness and 100 mm diameter; it was sliced from 100-mm-diameter and 200-mm-height cylindrical specimens. Moreover, 0.3 M of NaOH and 3% of NaCl solutions are used in positive and negative terminals, respectively, in the equipment setup cells represented in Fig. 4. The passage of electricity flow between the cells through the specimen is measured in terms of coulombs. The highest passage of current represents low resistance to chloride ionic penetration.

Open porosity test

As per ASTM C 642-06 [32], the open porosity test was conducted to determine the red mud concrete’s porous nature, and the size of the sample was considered 100 mm in diameter, 50 mm in thickness.

$$p = \frac{W_{ssd} - W_d}{W_{ssd} - W_w} \times 100\% \tag{1}$$

p = porosity, W_d = dry weight of specimen, W_{ssd} = saturated surface dry weight of specimen, W_w = wet weight of specimen.

Table 3 Mix proportions of red Mud-based concrete

Materials	Mix A					Mix B				
	A0RM	A5RM	A10RM	A15RM	A20RM	B0RM	B5RM	B10RM	B15RM	B20RM
Cement	432	410.4	388.8	367.2	345.6	450	427.5	405	382.5	360
Red mud (RM)	0	21.6	43.2	64.8	86.4	0	22.5	45	67.5	90
Silica fume (SF)	0	0	0	0	0	85.4	85.4	85.4	85.4	85.4
Fine aggregates	654	654	654	654	654	589	589	589	589	589
Coarse aggregates	1180	1180	1180	1180	1180	1180	1180	1180	1180	1180
Water	172	172	172	172	172	172	172	172	172	172
Superplasticizer	2.15	2.15	2.15	2.15	2.15	4.3	4.3	4.3	4.3	4.3

**Fig. 4** Experimental setup of rapid chloride permeability test

Sorptivity test

The sorptivity test was conducted to evaluate water penetration (with prescribed time) into the red mud concrete samples as per ASTM C1585-13 [33]. The size of the samples used for sorptivity was 50 mm thickness and 100 mm diameter. Wax was applied on all the specimen sides except on the surface, subjected to the penetration of water and sorptivity values calculated using Eq. (2).

$$S = \frac{\Delta w}{A \times d \times \sqrt{t}} \quad (2)$$

S = coefficient of sorptivity ($\text{mm}/\text{min}^{0.5}$), A = water exposed area of the specimen (mm^2), t = time (min), d = density of water ($10^{-3} \text{ g}/\text{mm}^3$).

Water absorption test

As per IS 1124-1974 [34], the water absorption test has been conducted on all concrete samples. Before testing, samples were heated in an oven at the temperature of 105°C to promise that no moisture should be present inside the concrete. Then, the sample was weighed, and it was considered as dry weight (W_d). Afterward, the samples were immersed completely in water for 24 h, the samples were taken out, and the surface was cleaned by using water absorbent paper. Once again, the samples were weighed and it was considered as wet weight (W_w). The percentage of water absorption was calculated by using Eq. (3).

$$W = \frac{W_w - W_d}{W_d} \times 100. \quad (3)$$

Accelerated corrosion test

An accelerated corrosion test (ACT) was conducted to identify the corrosion resistivity of RM concrete. Cylindrical samples of 100 mm diameter and 200 mm height with a 12-mm-diameter steel bar were cast for the test. The test setup consists of a 12-V DC power supply, stainless steel container, a data logger, test specimens with a container filled with a 3% concentrated NaCl solution. The positive charge cable was connected to a reinforcement bar (anode), and the negative charge cable was connected to a steel container (cathode). Figure 5 depicts the experimental setup of the accelerated corrosion test. The response of the current is continuously monitored and recorded by the data logger. The test was terminated when the rate of increase of corrosion current with time was negligible. It happens when the specimen achieves cracking.



Fig. 5 Experimental setup of accelerated corrosion test

Details of XRD and SEM

In this study, microstructural investigations, viz. scanning electron microscope, energy-dispersive spectroscope, and X-ray diffraction analysis, were conducted to red mud concrete and standard concrete samples. Rigaku mini flex 600 was used for XRD measurements with the following parameters; 40 kV of voltage and 15 mA of current, step scan of 0.0200°, scan range from 3° to 90° (2θ), and a scan speed of 100.00 deg/min with CuKα/1.541862 Å of wavelength. Powdered samples were considered for XRD analysis, and representative samples of 5 mm × 5 mm × 10 mm size were considered for scanning electron microscope and energy-dispersive spectroscope analysis. Gold sputtering was applied to all the samples before placing it into a scanning electron microscope, as concrete is a non-conductive material.

Results and discussion

Compressive strength

Table 4 shows the mechanical properties of red mud concrete for Mixes A and B. The compressive strength

Table 4 Compressive strength of red mud concrete

Age of curing	Mix A					Mix B				
	A0RM	A5RM	A10RM	A15RM	A20RM	B0RM	B5RM	B10RM	B15RM	B20RM
7D	30.16	33.65	35.67	34.54	31.27	52.1	54.5	59.9	56.17	53.2
28D	43.55	45.34	48.12	46.05	44.09	82.2	83.8	87.7	84.12	82.8
90D	48.25	55.61	59.75	53.79	52.18	84.2	92.4	103.7	99.8	89.1
150D	49.5	61.12	67.56	60.22	57.53	85.3	95.9	110	102.5	91.2

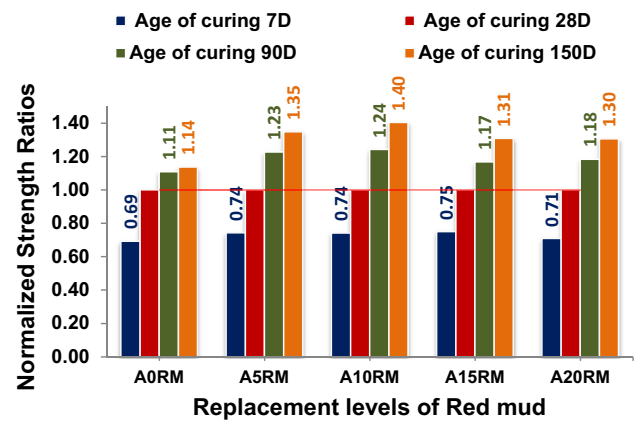


Fig. 6 Normalized strength ratios versus red mud replacement levels for Mix A

values are highest for 10% red mud replacement mixes (A10RM & B10RM). The aluminates in red mud accelerated the cement hydration; this effect led to greater early age strength than normal mixes. Figures 6 and 7 show the normalized ratios of compressive strength for Mixes A and B with different red mud replacement levels. Moreover, Mix A has shown significant strength enhancement with progress in the age of curing. This effect is due to the secondary pozzolanic activity between cementitious materials (cement and red mud). In contrast, Mix B with a low water–cement ratio has not shown strength enhancement to a great extent at later ages. It was attributed due to less availability of water for secondary pozzolanic activity than Mix A. Due to high alkalinity (pH > 12) nature, red mud accelerates the pozzolanic reaction between cementitious materials (cement and red mud) [1, 12, 20, 35]. After 10% of red mud replacement in concrete, the strength reduction was observed, but it is not lower than normal concrete mixes. At 15% and 20% of red mud replacement in concrete, compressive strength was reduced because of insufficient cement hydration due to the presence of higher red mud content at higher replacement. A similar justification was given by Cheng et al. [36]; red mud has a high specific surface area that absorbs more water in the concrete mix; it leads to the shortage of water for sufficient cement hydration.

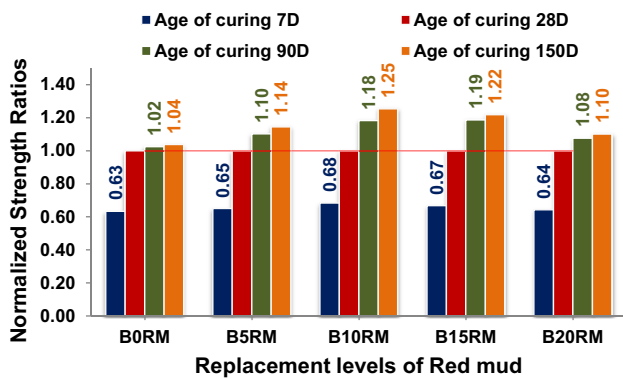


Fig. 7 Normalized strength ratios versus red mud replacement levels for Mix B

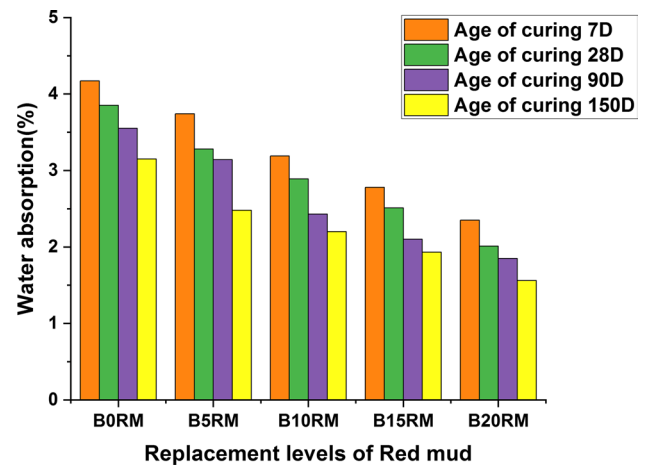


Fig. 9 Water absorption of Mix B red mud concrete

Water absorption test

Red mud concrete diminishes the percentage of water absorption with an increase in the replacement of red mud. The water absorption test was conducted after a specified age of curing, i.e., 7D, 28D, 90D, 150D. The thought of interest is to identify the water absorption resistance in red mud concrete with hydration advancement. Figures 8 and 9 illustrate the percentage of water absorption at various red mud replacement levels for Mixes A and B. After 7 days of curing, water absorption has reduced from 6.13% (A0RM) to 2.65% (A20RM) and 4.17% (B0RM) to 2.35% (B20RM). However, in the case of 150 days curing, water absorption was reduced from 2.73% (A0RM) to 1.83% (A20RM) and 3.15% (B0RM) to 1.56% (B20RM). The results illustrate that with an increase in curing age and with enhanced replacement level, the water absorption values are reduced. Red mud develops the pozzolanic activity at a later age also; it leads to minimizing connections between the pores. Another

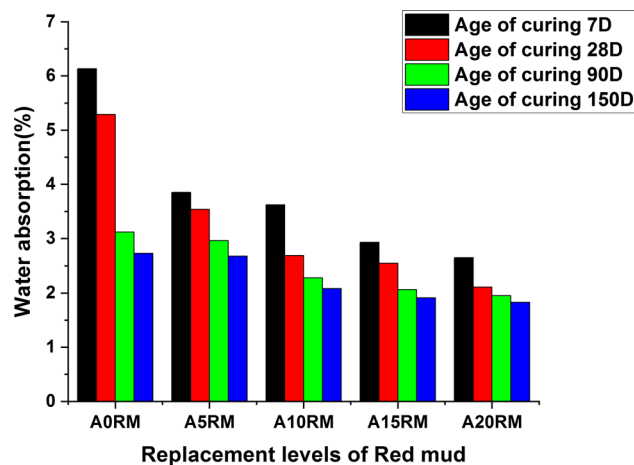


Fig. 8 Water absorption of Mix A red mud concrete

reason for reducing water absorption is the fineness of red mud particles (average particle size 14 μm); all micro-cracks and pores present in the concrete are sealed. Red mud can minimize the water absorption of concrete by its large specific surface area [37]. Manfro et al. 2014 [21] gave a similar reason; in the red mud-based cement hydration process, the higher Ca(OH)₂ crystals were broken into several small crystals and less oriented, which leads to minimization of pore connections and water absorption.

Sorptivity test

Water absorption through capillary suction was measured on red mud concrete samples and is represented in Figs. 10 and 11. The sorptivity values shown in Table 5 are observed to decrease with an increase in the level of red mud replacements in concrete. After 28 days of curing, the sorptivity values are reduced from 0.562 mm/min^{0.5} (A0RM) to 0.266 mm/min^{0.5} (A20RM) and 0.358 mm/min^{0.5} (B0RM) to 0.260 mm/min^{0.5} (B20RM), and this is attributed due to fineness of red mud which makes the concrete surface very dense by filling all the voids. This filling nature would help develop the continuous pozzolanic reaction between red mud and cement, enhancing the strength and durability characteristics of concrete at later ages. In the present study, micro-structure analysis revealed that replacement of red mud in concrete reduced sorptivity values because of C–S–H filled all the capillary pores during hydration. The sorptivity values are decreased with the addition of red mud in concrete because red mud fills voids and cracks in concrete [18, 38].

Open porosity test

Open porosity test was performed to understand the porosity of concrete with red mud addition. Table 6

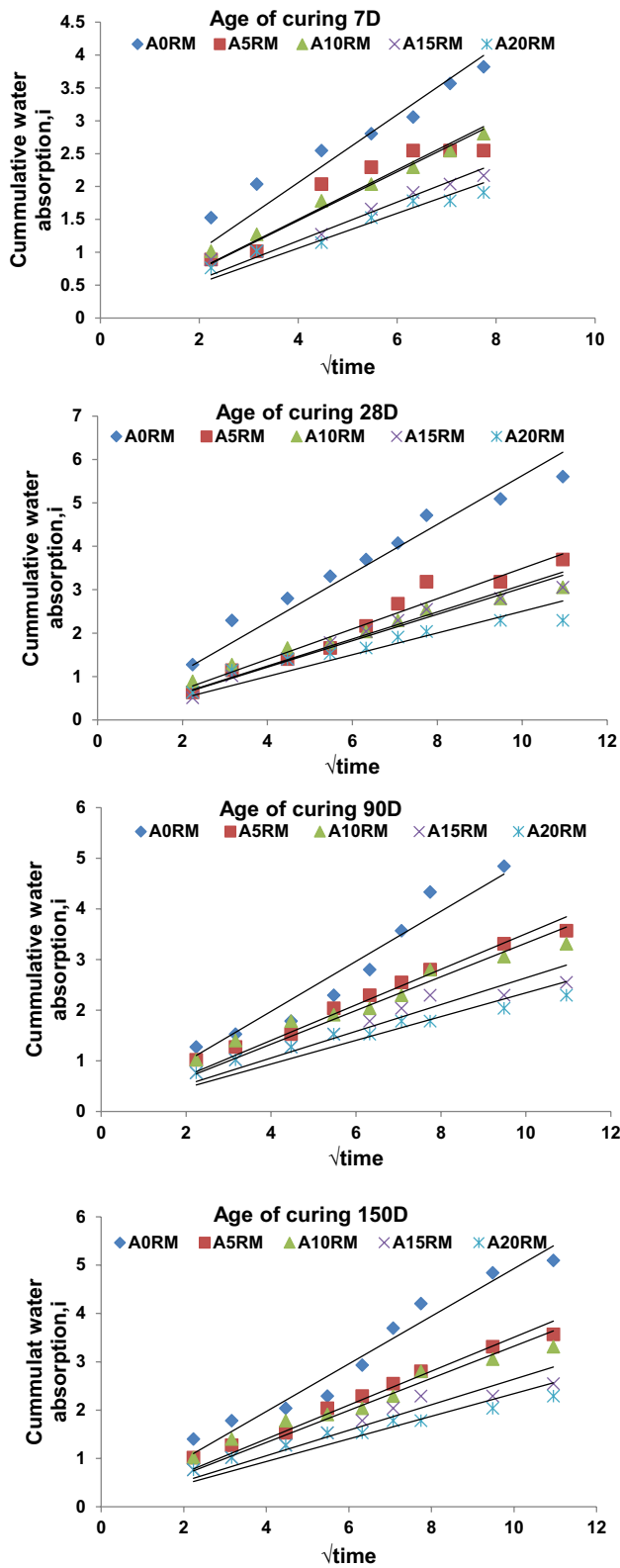


Fig. 10 Cumulative water absorption versus $\sqrt{\text{time}}$ for Mix A concrete

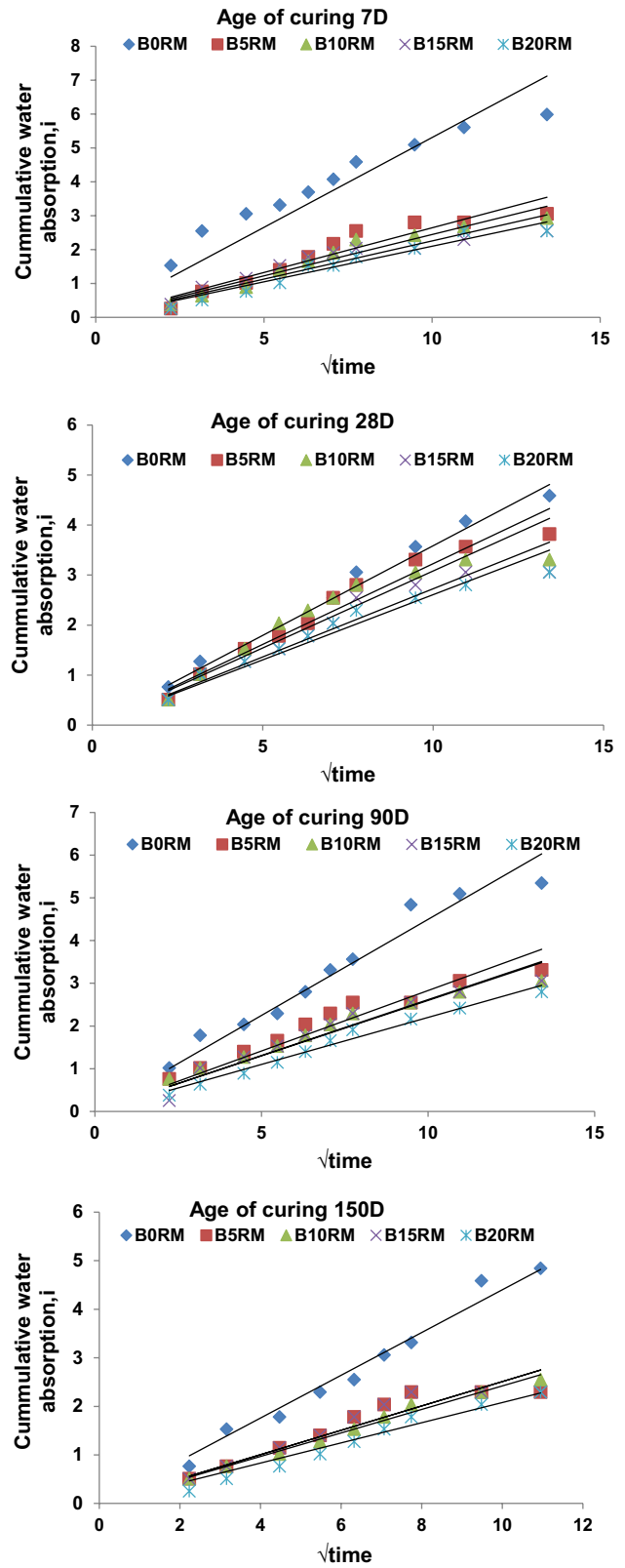


Fig. 11 Cumulative water absorption versus $\sqrt{\text{time}}$ for Mix B concrete

Table 5 Sorptivity values for red mud concrete

Age of curing	Mix A					Mix B				
	A0RM	A5RM	A10RM	A15RM	A20RM	B0RM	B5RM	B10RM	B15RM	B20RM
7D	0.515	0.375	0.352	0.294	0.265	0.530	0.264	0.244	0.255	0.209
28D	0.562	0.360	0.323	0.292	0.266	0.358	0.322	0.308	0.272	0.260
90D	0.493	0.350	0.332	0.263	0.243	0.449	0.283	0.261	0.229	0.220
150D	0.492	0.350	0.332	0.263	0.234	0.44	0.251	0.241	0.241	0.207

Table 6 Porosity (%) of red mud concrete

Age of curing	Mix A					Mix B				
	A0RM	A5RM	A10RM	A15RM	A20RM	B0RM	B5RM	B10RM	B15RM	B20RM
7D	6.13	5.47	4.42	2.93	2.65	4.7	4.6	3.4	3.02	2.56
28D	5.29	4.83	2.55	1.19	1.01	4.32	3.46	2.1	1.63	1.53
90D	5.06	4.36	2.13	1.16	1.02	3.79	3.24	1.47	1.31	1.20
150D	5.01	4.36	2.09	1.16	1	3.41	3.24	1.47	1.25	1.11

represents the porosity values of red mud concrete. In Mix A, porosity (%) reduced from 6.13(A0RM) to 2.65(A20RM) @7D, 5.29(A0RM) to 1.01(A20RM) @28D, 5.06 (A0RM) to 1.02(A20RM) @90D and 5.01(A0RM) to 1(A20RM)@150D. Mix B also exhibited similar kinds of results. The porosity of concrete reduced significantly with red mud in concrete. This effect is due to filling pores by C–S–H during hydration, which is observed in the micro-structure investigation in the present study (represented in Section “SEM–EDS analysis”). Moreover, another reason is the fineness of red mud, which fills the pore structure of concrete. A dense surface structure was formed due to red mud’s fineness, which reduces concrete porosity [18, 21, 35]. The similar tests, viz. Water absorption test, sorptivity test, and open porosity test, achieved similar results.

Rapid chloride penetration test

As per ASTM C1202-19 [31], the passage of chloride ions into RM concrete has been investigated in current work. Figures 12 and 13 present the total charge passed in standard and high-grade concrete mixes with different red mud replacement levels. As per experimental observations, the passage of coulombs was reduced from 2613 °C (A0RM) to 1168 °C (A20RM) and 2120 °C (B0RM) to 730 °C (coulombs) (B20RM) for 7 days curing completed specimens. As the age of curing progressed for both mixes, the current passed was moderately decreased for a different level of replacements of red mud concrete. The C–S–H fills most of the voids, and red mud particles fill a few more voids. The filling effect of RM particles in micropores in concrete diminishes the chloride ions penetration. Many studies [1, 18] reported that the reduction of chloride ions penetration

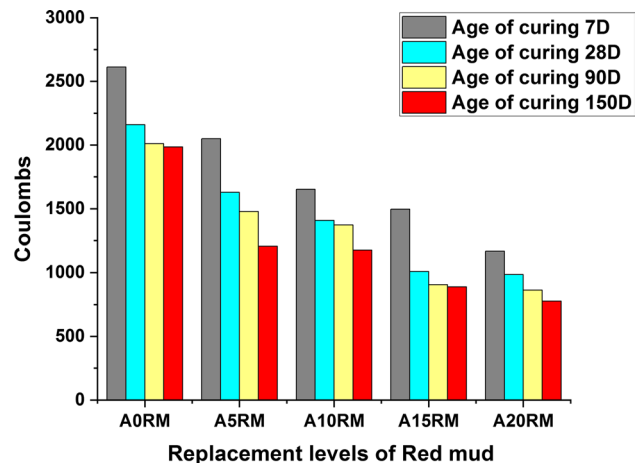


Fig. 12 Passage of coulombs Mix A red mud concrete

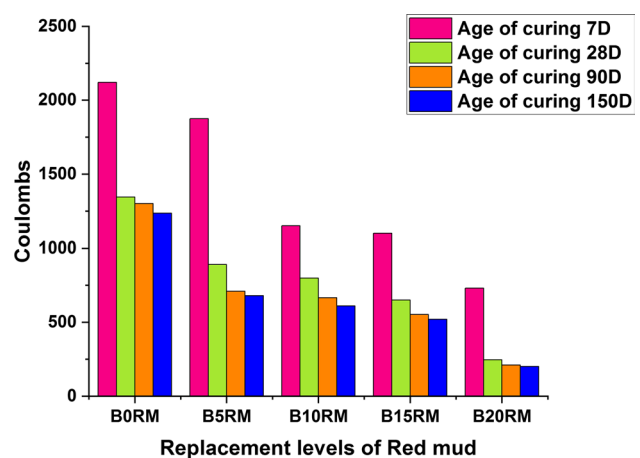


Fig. 13 Passage of coulombs for Mix B red mud concrete

and carbonation depth is because of fine RM particles and concluded similarly.

Accelerated corrosion test

In this study, an accelerated corrosion test (ACT) has been performed to identify the corrosion behavior in red mud concrete. Table 7 represents the rebar mass loss (%) due to corrosion. Red mud offers significant corrosion resistance with an increase in the replacement levels of red mud in concrete. Table 8 expresses the critical corrosion current and post-depassivation time for red mud concrete mixes at different ages. In Mixes A and B, the failure crack was observed after 18D @32.1 mA (A0RM), 30D @18.6 mA (A5RM), 37D @15.2 mA (A10RM), 40D @12.5 mA (A15RM), 41D @11.4 mA (A20RM) and 25D @22.3 mA (B0RM), 43D @14.8 mA (B5RM), 49D @11.5 mA (B10RM), 52D @10.2 mA (B15RM), 53D @8.6 mA (B20RM) of critical corrosion current after 28 days of curing age. On considering the rebar mass loss (%) with post-depassivation cracking time, it is understood that the samples with more mass loss exhibited less depassivation time, which is due to the less chloride ionic penetration resistance. On the other hand, the presence of higher content of red mud depicted more resistance to ionic penetration to the alkaline nature of red mud, which minimizes the depassivation of the reinforcement bar

surface against chloride ions ingress in concrete. Many studies gave similar reasons [9, 18, 39]. Red mud was the most promising corrosion inhibitor. The vigorous experimental investigation of Belén Díaz et al. [15] identified a drastic reduction in diffusivity values of chlorides and CO₂ for red mud added cement paste specimens. This reduction of chloride ion diffusivity in due to the presence of high alumina content in RM could trap chlorides and from Friedel’s salt. Figure 14 represents the failure of the samples due to corrosion.

Micro-level properties of red mud concrete

XRD analysis

X-ray diffraction analysis was conducted on red mud concrete samples of Mix A. Figure 15 presents the X-ray diffractograms of concrete of Mix A with different red mud replacement levels. The mineral phases identified for different mixes were quartz (SiO₂), larnite (Ca₂SiO₄), hatrurite (Ca₃SiO₅), portlandite (Ca(OH)₂), ettringite (Ca₆Al₂(SO₄)₃(OH)1226H₂O) and katoite (Ca₃Al₂(SiO₄)(OH)₈). Portlandite in red mud concrete helps to hold the alkali pore solution concentration during cement hydration and thus enhances the C–S–H gel formation. Katoite could

Table 7 Rebar mass loss (%) due to corrosion

Age of curing	Mix A					Mix B				
	A0RM	A5RM	A10RM	A15RM	A20RM	B0RM	B5RM	B10RM	B15RM	B20RM
7D	18.8	10.29	7.62	6.05	5.15	14.60	8.24	5.83	4.58	3.26
28D	14.60	6.74	5.55	4.94	3.48	9.55	5.61	3.33	2.19	1.74
90D	12.35	7.3	5.55	4.39	2.9	7.86	4.49	3.86	1.64	1.73
150D	11.23	6.17	5	4.39	2.32	7.86	4.49	3.33	1.64	1.74

Table 8 Failure crack observations

Age of curing	A0RM	A5RM	A10RM	A15RM	A20RM	B0RM	B5RM	B10RM	B15RM	B20RM
7D										
Critical corrosion current (mA)	48.9	23.4	21.3	17.5	16.2	29.3	20.6	19.2	15.4	13.2
Post-depassivation time (days)	14	23	31	36	39	19	28	33	40	45
28D										
Critical corrosion current (mA)	32.1	18.6	15.2	12.5	11.4	22.3	14.8	11.5	10.2	8.6
Post-depassivation time (days)	18	30	37	40	41	25	43	49	52	53
90D										
Critical corrosion current (mA)	25.6	15.3	13.8	11.2	9.1	20.5	15.7	9.3	8.7	7
Post-depassivation time (days)	20	36	41	45	47	24	49	54	55	62
150D										
Critical corrosion current (mA)	23.7	14.6	12.1	11.2	9	18.3	13.1	8.6	7.3	5
Post-depassivation time (days)	24	40	41	44	47	25	53	57	57	65



Fig. 14 Failure pattern of the samples

1.Larnite, 2.Portlandite, 3. Katoite, 4.Ettringite, 5.Calcium carbonate, 6.Hatruirite

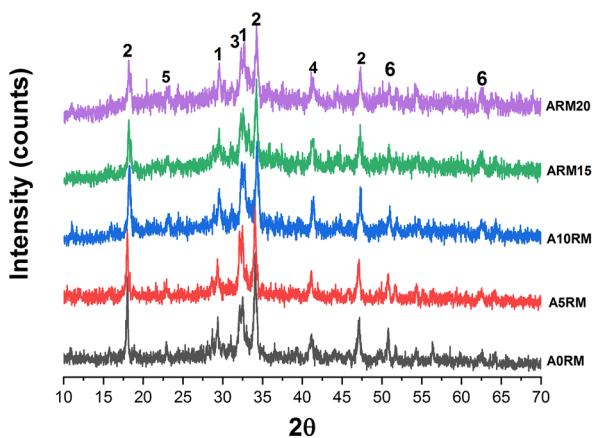


Fig. 15 X-ray diffractograms for RM concrete

enhance the durability of concrete in terms of more heat liberation; meanwhile, it reduces the presence of sulfate and makes the concrete stable [15, 40]. Quartz reacts with calcium oxide in the cement hydration and helps in the formation of C–S–H gel. In the red mud concrete, the presence of larnite and hatruirite gives clear evidence for C–S–H gel formation, making the concrete achieve strength characteristics. In the present study, a higher percentage of larnite and hatruirite was observed at RM 10% mix, and this is the reason for high strength, as shown in Table 9.

Table 9 XRD hydration compounds (weight%)

Hydration compounds	Age of curing 28 days				
	A0RM	A5RM	A10RM	A15RM	A20RM
Portlandite	24.5	24.6	24.4	25.6	22.8
Ettringite	3.3	3.7	3.3	3.3	3.9
Katoite	8.9	9.2	8.1	9.6	10.5
Calcium carbonate	8.1	5.1	3.2	3.1	6
Larnite	25.7	26.1	27.5	26.8	26.1
Hatruirite	29.5	31.3	33.5	31.6	30.7
Total	100	100	100	100	100

SEM–EDS analysis

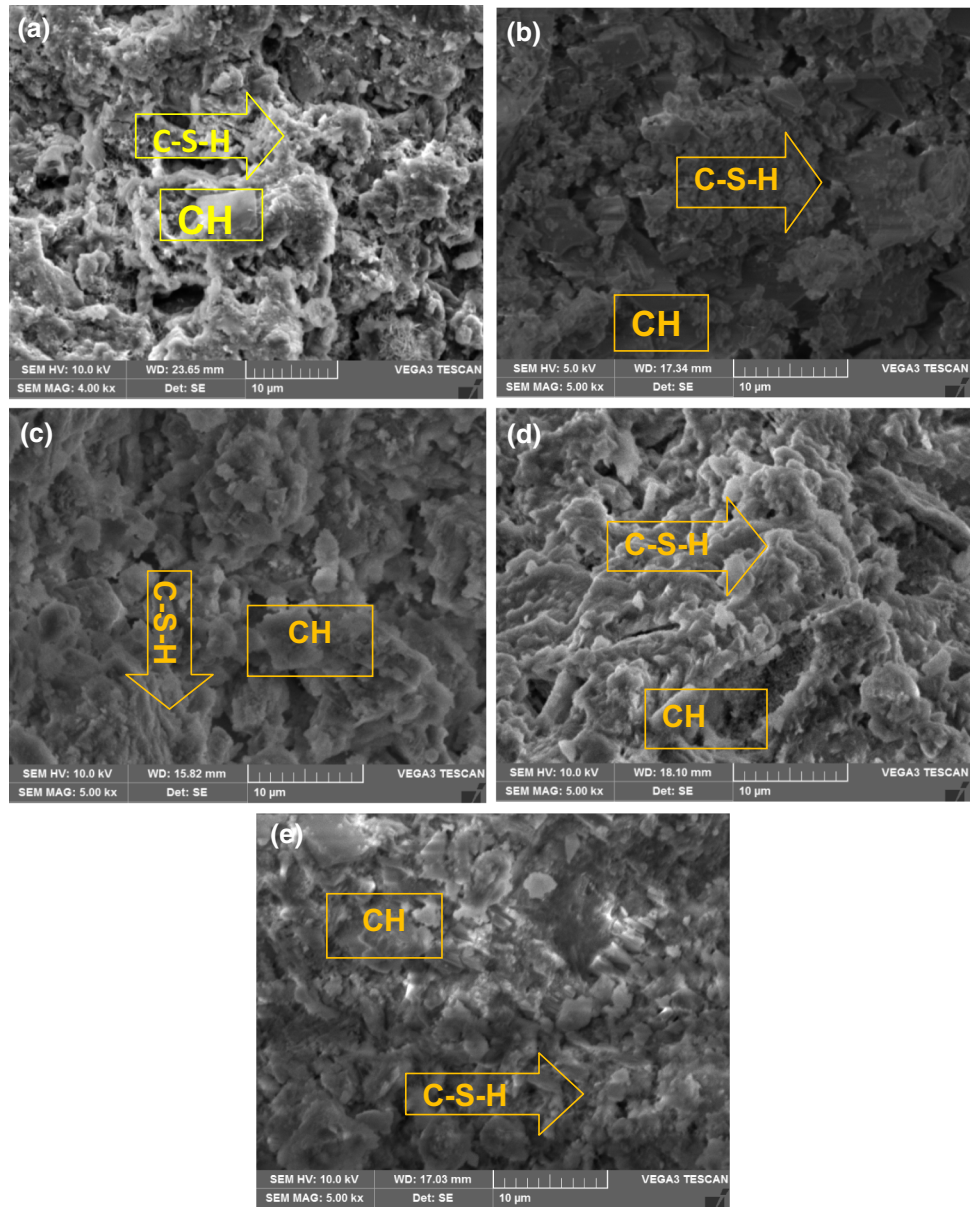
For knowing the morphological behavior of red mud concrete, micro-level investigations were conducted with a scanning electron microscope (SEM) and energy-dispersive spectroscope (EDS) analysis for elemental composition. Figure 16a–e represents the SEM images of Mix A (standard grade) concrete with different levels of replacement of red mud. It is identified from SEM images that increasing the replacement levels of red mud in concrete results in dense structure formation. The finer particles of red mud occupied the pores in the concrete and decreased the porosity of concrete. Figure 17a–e represents the energy-dispersive spectroscopy analysis of all mix samples. The Ca/Si ratio range of 0.8 to 2.5 is the evidence for C–S–H gel presence in concrete [41]. In the present study, Ca/Si ratios are 1.13, 0.99, 0.95, 1.01, and 1.08 at red mud replacement of 0%, 5%, 10%, 15%, and 20%, respectively. Based on the results, 10% of red mud replacement in concrete has shown lesser Ca/Si ratio than other mixes. The lower the Ca/Si ratio, the higher the C–S–H gel formation, and the higher the Ca/Si ratio, the lower the C–S–H gel formation [1], which is the reason for the higher strength observed at 10% red mud replaced mix.

Conclusions

The following conclusions were drawn after the evaluation of the durability and micro-level properties of RM concrete.

- Red mud contains a higher percentage of alumina, which accelerated the cement hydration, and this is the reason for achieving high strength at an early age than normal concrete.

Fig. 16 Scanning electron microscope images of **a** A0RM, **b** A5RM, **c** A10RM, **d** A15RM, **e** A20RM



- Both mixes (Mixes A and B) have considerable strength enhancement with the progression in an age of curing; but lesser strength increment was observed in Mix B than in Mix A. It might be due to insufficient water availability for secondary pozzolanic activity.
- The 10% replacement of RM has shown higher compressive strength; the reason for the strength increment was the high alkaline (pH > 12) nature of red mud accelerates the pozzolanic reaction between the cementitious materials.
- The fineness of red mud particles sealed all the micro-cracks and pores present in concrete because C-S-H filled all the capillary pores during hydration, resulting in dense concrete. Tests, viz. Water absorption, sorptivity, and open porosity identified the effectiveness of red mud concrete.
- The filler effect of RM diminished chloride permeability, and the high alkalinity of RM more strengthen the

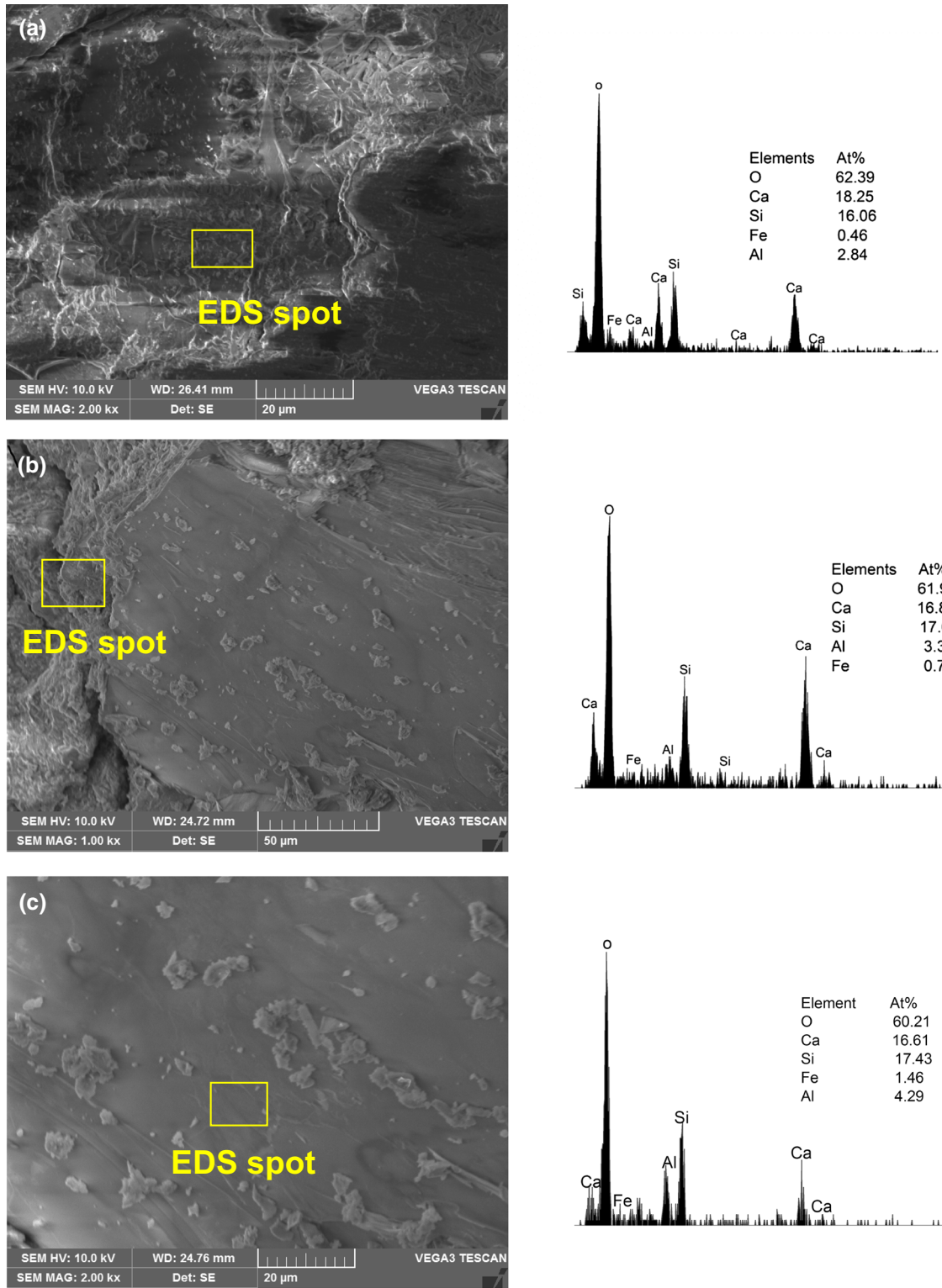


Fig. 17 Energy-dispersive spectroscopy results for a A0RM, b A5RM, c A10RM, d A15RM, e A20RM

reinforcement surface passive layer, which enhanced the corrosion resistivity of reinforced concrete.

- In both mixes, 10% RM replacement samples showed a higher percentage of larnite, hatrurite, and low Ca/Si ratio. These are the reasons for achieving high strength.

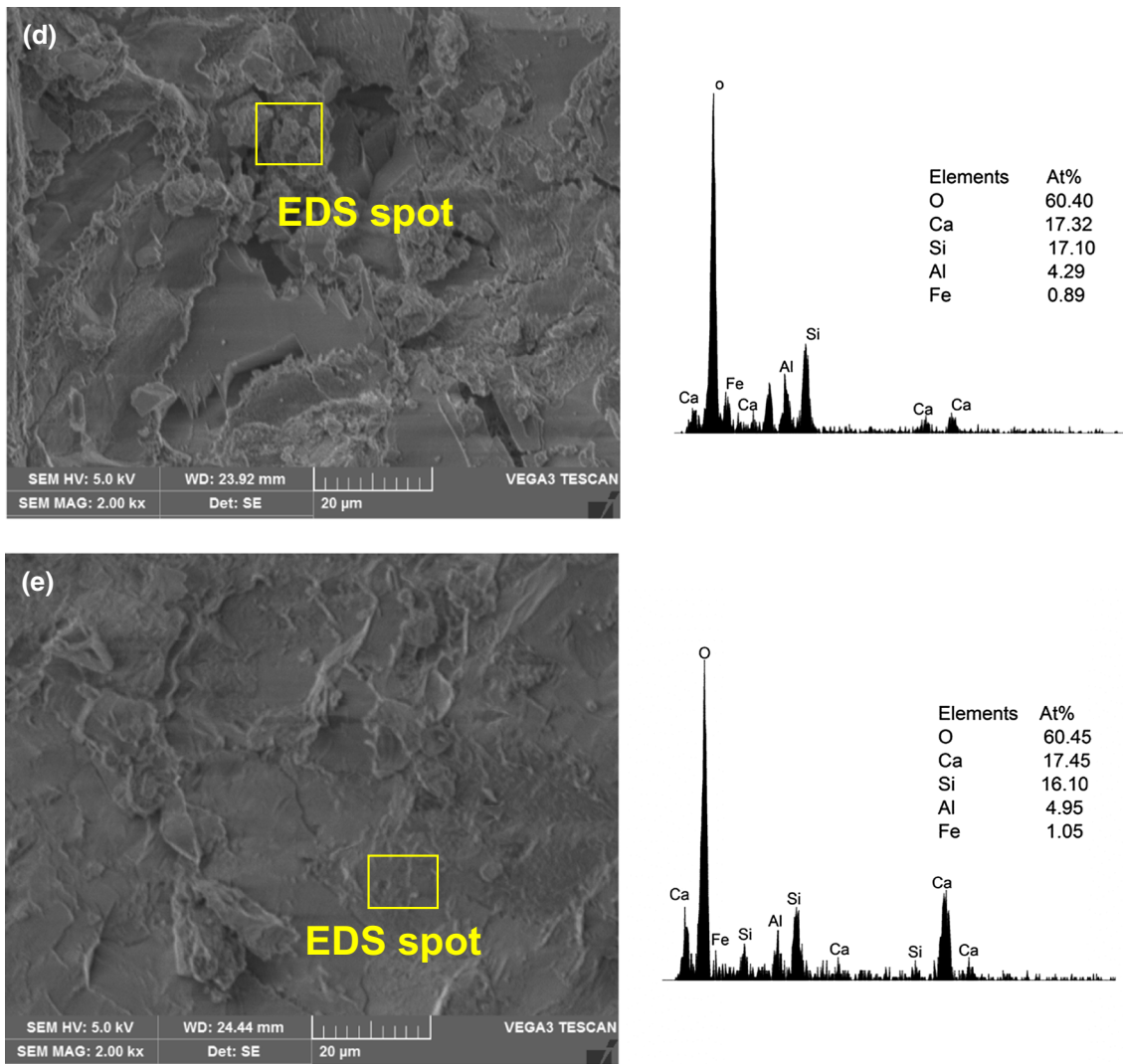


Fig. 17 (continued)

Acknowledgements The authors are thankful to the Centre of Excellence for Advanced Materials, Manufacturing, Processing, and Characterization for allowing to conduct Microstructural analysis, Vignan’s Foundation for Science, Technology and Research, Guntur, Andhra Pradesh, India, 522213.

Compliance with ethical standards

Conflict of interest The authors declare that they have no conflict of interest.

References

1. Venkatesh C, Ruben N, Chand MSR (2020) Red mud as an additive in concrete: comprehensive characterization. *J. Korean Ceram. Soc.* 57(3):281–289. <https://doi.org/10.1007/s43207-020-00030-3>

2. Abdel-Raheem M, Santana LG, Cordava MP, Martínez BO (2017) Uses of red mud as a construction material. In: AEI 2017, pp 388–399

3. Venkatesh C, Chand MSR, Ruben N (2019) A state of the art on red mud as a substitutional cementitious material. *Ann Chim Sci Mater* 43(2):99–106

4. Ujaczki É, Klebercz O, Feigl V, Molnár M, Magyar Á, Uzinger N, Gruiz K (2015) Environmental toxicity assessment of the spilled Ajka red mud in soil microcosms for its potential utilisation as soil ameliorant. *Periodica Polytech Chem Eng* 59(4):253–261

5. Dentoni V, Grosso B, Massacci G (2014) Environmental sustainability of the alumina industry in Western Europe. *Sustainability* 6(12):9477–9493

6. Metilda DL, Selvamony C, Anandakumar R, Seeni A (2015) Investigations on optimum possibility of replacing cement partially by redmud in concrete. *Sci Res Essays* 10(4):137–143

7. Shakir AA, Naganathan S, Mustapha KNB (2013) Development of bricks from waste material: a review paper. *Aust J Basic Appl Sci* 7(8):812–818

8. Bhasin S, Chandra N (2004) Studies on sintering behavior of pyrophyllite based ceramic tiles using di-potassium phosphatic binder. *Silic Ind* 69(1–2):14–18
9. Venkatesh C, Mohiddin SK, Ruben N (2019) Corrosion inhibitors behaviour on reinforced concrete—a review. In: Das B, Neithalath N (eds) *Sustainable construction and building materials*. Springer, Singapore, pp 127–134
10. Sawant AB, Kumthekar MB, Sawant SG, Mud AR (2013) Utilization of neutralized red mud (industrial waste) in concrete. *Int J Invent Eng Sci (IJIES)* 1(2):9–13
11. Shetty KK, Nayak G, Shetty R (2014) Self compacting concrete using red mud and used foundry sand. *Int J Res Eng Technol* 3(3):708–711
12. Ribeiro DV, Silva AS, Labrincha JA, Morelli MR (2013) Rheological properties and hydration behavior of Portland cement mortars containing calcined red mud. *Can J Civ Eng* 40(6):557–566
13. Yang X, Zhao J, Li H et al (2017) Recycling red mud from the production of aluminium as a red cement-based mortar. *Waste Manag Res* 35:1–8
14. Senff L, Modolo RCE, Silva AS, Ferreira VM, Hotza D, Labrincha JA (2014) Influence of red mud addition on rheological behavior and hardened properties of mortars. *Constr Build Mater* 65:84–91
15. Díaz B, Freire L, Nóvoa XR, Pérez MC (2015) Chloride and CO₂ transport in cement paste containing red mud. *Cement Concr Compos* 62:178–186
16. Babu UR, Kondraivendhan B (2020) Influence of bauxite residue (red mud) on corrosion of rebar in concrete. *Innov Infrastruct Solut* 5(3):1–10
17. Ribeiro DV, Labrincha JA, Morelli MR (2012) Effect of the addition of red mud on the corrosion parameters of reinforced concrete. *Cem Concrete Res* 42(1):124–133
18. Raja RR, Pillaib EP, Santhakumarc AR (2013) Effective utilization of redmud bauxite waste as a re-placement of cement in concrete for environmental conservation. *Ecol Environ Conserv* 19(1):247–255
19. Díaz B, Joiret S, Keddami M, Nóvoa XR, Pérez MC, Takenouti H (2004) Passivity of iron in red mud's water solutions. *Electrochim Acta* 49(17–18):3039–3048
20. Ribeiro DV, Labrincha JA, Morelli MR (2011) Potential use of natural red mud as pozzolan for Portland cement. *Mater Res* 14(1):60–66
21. Manfroi EP, Cheriaf M, Rocha JC (2014) Microstructure, mineralogy and environmental evaluation of cementitious composites produced with red mud waste. *Constr Build Mater* 67:29–36
22. Liu RX, Poon CS (2016) Utilization of red mud derived from bauxite in self-compacting concrete. *J Clean Prod* 112:384–391
23. Liu X, Zhang N, Sun H, Zhang J, Li L (2011) Structural investigation relating to the cementitious activity of bauxite residue—red mud. *Cem Concr Res* 41(8):847–853
24. ASTM C150/C150M-16e1 (2016) Standard specification for Portland cement. ASTM International, West Conshohocken, PA
25. BIS, IS 4031-I (1996) Specifications for method of physical tests for hydraulic cement. Bureau of Indian Standards, New Delhi
26. BIS, IS 383-2016 (2016) Specification for coarse and fine aggregates from natural sources for concrete. Bureau of Indian Standards, New Delhi
27. ASTM, ASTM C494 (2019) Standard specification for chemical admixtures for concrete. ASTM, West Conshohocken
28. BIS, IS 10262–2019 (2019) Specification for mix design guidelines for concrete. Bureau of Indian Standards, New Delhi
29. BIS, IS 456-2000 (2000) Specification for plain and reinforced concrete. Bureau of Indian Standards, New Delhi
30. BSI, BS 12390-3:2009 (2009) Testing hardened concrete. Compressive strength of test specimens. British Standards Institution, London
31. ASTM C1202-12 (2012) Standard test method for electrical indication of concrete's ability to resist chloride ion penetration. ASTM International, West Conshohocken, PA
32. ASTM C 642-06 (2006) Standard Test method for density, absorption and voids in hardened concrete. ASTM International, West Conshohocken, PA
33. ASTM C1585-13 (2013) Standard test method for measurement of rate of absorption of water by hydraulic-cement concretes. ASTM International, West Conshohocken, PA
34. BIS, IS 1124-1974 (1974) Specification for water absorption for concrete. Bureau of Indian Standards, New Delhi
35. Ribeiro DV, Labrincha JA, Morelli MR (2010) Use of red mud as addition for portland cement mortars. *J Mater Sci Eng* 4(8):1–8
36. Cheng X, Yang X, Zhang C, Gao X, Yu Y, Mei K, Zhang C (2019) Effect of red mud addition on oil well cement at high temperatures. *Adv Cem Res*:1–11
37. Venkatesh C, Nerella R, Chand MSR (2019) Comparison of mechanical and durability properties of treated and untreated red mud concrete. *Mater Today: Proc* 27:284–287
38. Ribeiro DV, Labrincha JA, Morelli MR (2011) Chloride diffusivity in red mud-ordinary Portland cement concrete determined by migration tests. *Mater Res* 14(2):227–234
39. Tang WC, Wang Z, Donne SW, Forghani M, Liu Y (2019) Influence of red mud on mechanical and durability performance of self-compacting concrete. *J Hazard Mater* 37:120802
40. Tang WC, Wang Z, Liu Y, Cui HZ (2018) Influence of red mud on fresh and hardened properties of self-compacting concrete. *Constr Build Mater* 178:288–300
41. Sri Rama Chand M, Rathish Kumar P, Swamy Naga Ratna Giri P, Rajesh Kumar G (2018) Performance and microstructure characteristics of self-curing self-compacting concrete. *Adv Cem Res* 30(10):451–468